

T. MOHRI\*, S. OHISHI\*

## GLASS TRANSITION STUDIED BY CLUSTER VARIATION METHOD

### ANALIZA PRZEMIANY W SZKŁO METALICZNE Z ZASTOSOWANIEM METODY WARIACJI KLASTERÓW

Thermodynamics and kinetics frameworks of Glass transition are studied by Cluster Variation and Path probability Methods. Generalized phase diagram and cooling curve obtained by these calculations reproduce the essential features of the glass transition. These results are compared with the ones obtained from free energy model by Granato. The extension of the present model to incorporate structural information of glass by Continuous Displacement Cluster Variation Method is briefly discussed.

**Keywords:** glass transition, Cluster Variation Method, Path Probability Method, ideal glass transition temperature, Continuous Displacement Cluster Variation method

Analizowane są ramowe opracowania termodynamiki i kinetyki przemiany w szkło metaliczne z zastosowaniem metody wariacji klasterów oraz metody ścieżki prawdopodobieństwa. Uogólniony diagram fazowy i krzywa stygnięcia używane tymi metodami obliczeniowymi odtwarzają istotne cechy przemiany w szkło metaliczne. Wyniki te są skonfrontowane z tymi jakie otrzymuje się z modelu energii swobodnych opracowanego przez Granato. Krótko omówiono rozwinięcie prezentowanego modelu celem włączenia go do informacji strukturalnych o szkłe metalicznym przy zastosowaniu metody Ciągłego Zastępowania Metody Wariacji Kalsterów.

## 1. Introduction

Bulk Metallic Glass (BMG) has been attracting broad attentions for its superior mechanical, physical and anti-corrosion properties. Most of the studies on BMG, however, have been directed towards the development of a new class of BMG with better properties, and theoretical investigation of thermodynamic stabilities and their correlation with atomistic structures are still behind the satisfactory level.

Cluster Variation Method (hereafter CVM) [1] has been recognized as one of the most reliable theoretical tools in dealing with phase equilibria of a given alloy, and by combining with electronic structure total energy calculations, even first-principles studies of alloy phase equilibria have been successfully attempted [2].

Recently, one of the authors (TM) [3-6] has been attempting to extend the CVM to describe thermodynamics of Crystal-Glass (CG) transition, and calculated results were well summarized in the *generalized phase diagram* in which relevant stable and metastable phases are displayed along with loci of various characteristic

temperatures. It has been also found that the *ideal glass transition temperature* is equivalent to the *spinodal ordering temperature* in the Order-Disorder (OD) transition. The essential distinction between spinodal ordering and glass transition, however, is emphasized in the context of kinetics which plays an essential role in the latter transition.

One of the advantageous features of the CVM is the expandability to kinetics. In fact, Kikuchi devised Path Probability Method (hereafter PPM) [7] as the natural extension of the CVM to time domain and various ordering and relaxation kinetics towards equilibrium state have been investigated by combining CVM and PPM [2]. One of the present authors (TM) employed PPM to investigate cooling behavior of CG system and showed that the order parameter which characterizes the state of the system is frozen as approaching the ideal glass transition temperature [8]. Thereby, both the thermodynamics and kinetics frameworks of CG transition are consistently described by the CVM and PPM.

A deficiency of the conventional CVM has been pointed out in dealing with OD system. When the mix-

\* DIVISION OF MATERIALS SCIENCE AND ENGINEERING, GRADUATE SCHOOL OF ENGINEERING, HOKKAIDO UNIVERSITY, SAPPORO, 060-8628 JAPAN

ture of two kinds of species with large difference in atomic size is dealt, OD transition temperatures are considerably overestimated. Such inconvenience is ascribed to the neglect of local lattice distortion effects in the conventional CVM. In fact, in the conventional CVM, the Bravais lattice symmetry is assumed to be maintained everywhere in the lattice, and only uniform expansion/contraction is allowed. In order to overcome the inconveniences, Continuous Displacement CVM (CDCVM) has been developed by Kikuchi [9] as the extension of his study of liquid phase. In the CDCVM, atoms are allowed to displace to off-Bravais lattice point, leading to the reduction of the internal energy.

The capability of incorporating the additional freedom of atomic displacements implies that a geometrically disordered system in addition to the configurationally disordered phase can be handled. In fact, the motivation of the application of CDCVM to CG transition is ascribed to this point. Hence, in addition to the studies of thermodynamics and kinetics of CG transition, one would explore the structural aspects of the glass, namely the local atomic arrangements. Although the actual application of the CDCVM to CG transition is still away from the satisfactory level, various preliminary calculations on a two dimensional system has been attempted [10-14].

In the present report, CVM studies of CG transition performed by the authors' group are reviewed. The organization of the present report is as follows. In the next section, theoretical frameworks of the CVM and the application to CG transition is introduced. In the third section, kinetics studies of the CG transition by PPM is outlined. Two major results are reproduced from the previous studies; one is a generalized phase diagram [3-6] by the CVM and the other is the cooling curve [8] obtained by the PPM. In the fourth section, the free energy model of CG transition by Granato [15] which has a versatile applicability is introduced and calculated results based on the free energy are compared with the ones by CVM. Then, in the final section, CDCVM is introduced and its implication to the future studies of CG transition is discussed.

## 2. Thermodynamics of CG transition and Cluster Variation Method

The basic idea of the Cluster Variation Method (CVM) is to approximate the configurational freedom of atomic arrangement with a finite set of atomic clusters. The accuracy of the CVM is generally determined by the largest cluster, *basic cluster*, involved in the free energy. In the conventional applications of the CVM for fcc-based systems, a common practice is to employ tetra-

hedron approximation [16] in which nearest neighbor tetrahedron cluster is adopted as a basic cluster and the free energy of a L1<sub>0</sub> ordered phase, for instance, is given by

$$F^{L10} = \frac{1}{2} \cdot N \cdot \sum_{i,j} e_{ij} \cdot (y_{ij}^{\alpha\alpha} + 4y_{ij}^{\alpha\beta} + y_{ij}^{\beta\beta}) - k_B T \cdot \ln \frac{\left\{ \prod_{i,j} (N y_{ij}^{\alpha\alpha})! \right\} \left\{ \prod_{i,j} (N y_{ij}^{\alpha\beta})! \right\}^4 \left\{ \prod_{i,j} (N y_{ij}^{\beta\beta})! \right\} N!}{\left\{ \prod_i (N x_i^\alpha)! \right\}^{5/2} \left\{ \prod_i (N x_i^\beta)! \right\}^{5/2} \left\{ \prod_{i,j,k,l} (N w_{ijkl}^{\alpha\alpha\beta\beta})! \right\}^2}, \quad (1)$$

where  $x_i$ ,  $y_{ij}$  and  $w_{ijkl}$  are cluster probabilities of finding atomic arrangement specified by subscript(s) on a point, pair and tetrahedron clusters, respectively, the superscripts  $\alpha$  and  $\beta$  specify the sublattices,  $k_B$  the Boltzmann constant,  $T$  the temperature,  $N$  the total number of lattice point, and  $e_{ij}$  is the atomic pair interaction energy between species  $i$  and  $j$ . It should be emphasized that the choice of the L1<sub>0</sub> ordered phase for the free energy of the present study does not have any significant meaning except that the L1<sub>0</sub>-disorder transition is of the first order which is the basic requirement for the study of the liquid crystalline transition. In fact, the configurational information of the L1<sub>0</sub> ordered phase arising from short range orders described by pair and tetrahedron cluster probabilities are smeared out as will be seen shortly.

It has been amply demonstrated that the cluster probabilities are mutually dependent through normalization and geometrical conditions, and it is more convenient to employ correlation functions [2] instead of cluster probabilities, since correlation functions form a set of independent configurational variables. Hence, the free energy formula given above is formally rewritten as

$$F^{L10} = F(T, \{e_{ij}\}; x_i^\alpha, x_i^\beta, y_{ij}^{\alpha\alpha}, y_{ij}^{\alpha\beta}, y_{ij}^{\beta\beta}, w_{ijkl}^{\alpha\alpha\beta\beta}) = \hat{F}^{L10}(T, \{e_{ij}\}; \xi_1^\alpha, \xi_1^\beta, \xi_2^{\alpha\alpha}, \xi_2^{\alpha\beta}, \xi_2^{\beta\beta}, \xi_3^{\alpha\alpha\beta}, \xi_3^{\alpha\beta\beta}, \xi_4^{\alpha\alpha\beta\beta}), \quad (2)$$

where  $\xi_i$  is the  $i$ -body correlation function and the superscript indicates sublattice(s). The number of independent correlation functions are reduced due to the symmetry of the L1<sub>0</sub> ordered phase which claims  $\xi_1^\beta = -\xi_1^\alpha$ ,  $\xi_2^{\alpha\alpha} = \xi_2^{\beta\beta}$ , and  $\xi_3^{\alpha\beta\beta} = -\xi_3^{\alpha\alpha\beta}$  at a fixed 1:1 stoichiometric composition. Hence, the final form of the free energy is written as

$$F^{L10} = F(T, \xi_1^\alpha, \xi_2^{\alpha\alpha}, \xi_2^{\alpha\beta}, \xi_3^{\alpha\alpha\beta}, \xi_4^{\alpha\alpha\beta\beta}). \quad (3)$$

Among these five correlation functions, the point correlation function,  $\xi_1^\alpha (= x_A^\alpha - x_A^\beta)$ , serves as a Long Range Order parameter (LRO), while the rest of the correlation functions are Short Range Order parameters (SRO).

By minimizing the free energy,  $F^{L10}$ , with respect to all the SRO parameters for a given set of  $T$  and  $\xi_1^\alpha$ , one obtains the free energy expression formally given by,

$$F^{*L10} = f(T, \eta), \tag{4}$$

where point correlation function  $\xi_1^\alpha$  in eq.(3) is replaced by  $\eta$ . It is noted that  $\eta$  represents an amount of defects which induce crystal liquid transition, and  $\eta = 0.0$  and  $1.0$  are assigned to perfect solid and liquid phases, respectively, while the finite value of  $\eta$  suggests a defective crystal.

The calculated results are summarized in the generalized phase diagram shown in Fig.1[5,6] which indicates free energy contour lines, and stable regions of liquid (L), crystal (C), super-cooled liquid (SCL) and glass (G) are identified between the temperature loci of free

energy minimum ( $T_{eq}$ ), free energy maximum ( $T_{peak}$ ), and  $T_0$  temperature. The temperature axis is normalized with respect to the melting temperature,  $T_{melt}$ , at which the free energies of crystal and liquid becomes identical. The horizontal axis,  $\eta$ , represents the amount of defects as mentioned above. The essential quantity in CG transition is the ideal glass transition temperature,  $T_K$ , which was identified to be equivalent to the spinodal ordering temperature [17,18] of OD transition and is determined to be  $0.861$  at  $\eta = 0.976$  at which the entropies of liquid phase becomes identical with that of the defective crystal ( $\eta=0.976$ ), and a tri-critical point is formed in the generalized phase diagram. It is worth pointing out that  $T_0$  is the temperature at which the free energies of liquid and defective crystal become equivalent, hence the locus of  $T_0$  in Fig.1 can be seen as the melting temperature of a defective crystal characterized by  $\eta$ .

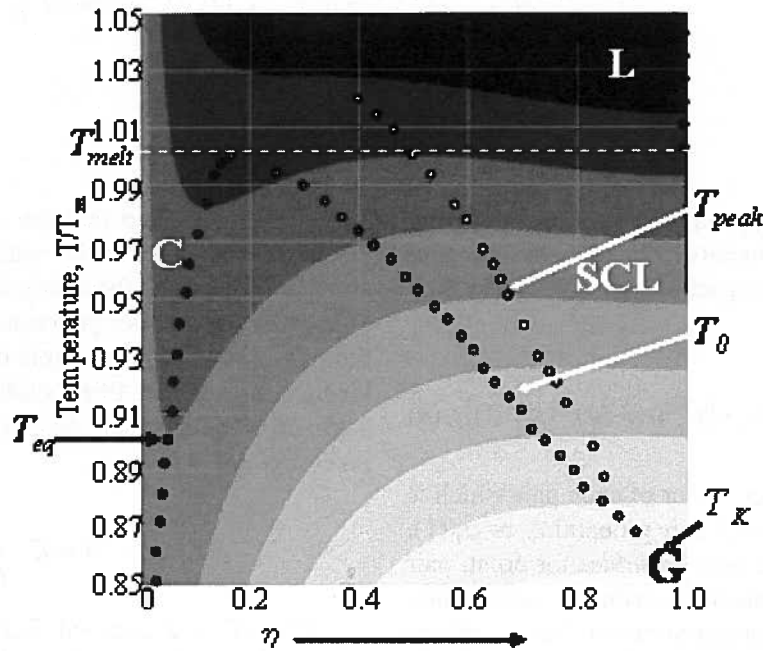


Fig. 1. Generalized phase diagram. L, C, SCL and G indicate liquid, crystal, super-cooled liquid and glass regions, respectively.  $T_{eq}$  is the locus of minimum of the free energy at each temperature,  $T_{melt}$  is the melting temperature by which the temperature axis is normalized,  $T_{peak}$  is the locus of maximum of free energy at each temperature and the free energy of a defective crystal becomes equivalent with that of liquid at  $T_0$ .  $T_K$  is the ideal glass transition temperature[5,6]

### 3. Kinetics of CG transition and Path Probability Method

As was mentioned in the Introduction, Path Probability Method (PPM) was devised as the natural extension of the Cluster Variation Method to time domain.

Hence, there are correspondences of key quantities appearing in CVM and PPM. The counter part of the free energy of the CVM is the *Path Probability Function (PPF)*,  $P$ , in PPM which is given as the product of the following three terms,

$$P_1 = \prod_{\delta=\alpha}^{\beta} (\theta \cdot \Delta t)^{\frac{N}{2} \cdot X_{1,i}^{\delta,\delta}} (\theta \cdot \Delta t)^{\frac{N}{2} \cdot X_{i,1}^{\delta,\delta}} (1 - \theta \cdot \Delta t)^{\frac{N}{2} \cdot X_{1,i}^{\delta,\delta}} (1 - \theta \cdot \Delta t)^{\frac{N}{2} \cdot X_{i,1}^{\delta,\delta}} \tag{5}$$

$$P_2 = \exp\left(-\frac{\Delta E}{2k_B T}\right), \quad (6)$$

and

$$P_3 = k_B \cdot \ln \frac{\left\{ \prod_{i,j} (NY_{ij,kl}^{\alpha\alpha})! \right\} \left\{ \prod_{i,j} (NY_{ij,kl}^{\alpha\beta})! \right\}^4 \left\{ \prod_{i,j} (NY_{ij,kl}^{\beta\beta})! \right\} N!}{\left\{ \prod_i (NX_{i,j}^{\alpha})! \right\}^{5/2} \left\{ \prod_i (NX_{i,j}^{\beta})! \right\}^{5/2} \left\{ \prod_{i,j,k,l} (NW_{ijkl,mnop})! \right\}^2}, \quad (7)$$

where  $\theta$  is the spin flipping probability per unit time that may correspond to the diffusivity of an alloy system, and  $\Delta E$  is the change of the internal energy during the time interval  $\Delta t$  given by

$$\Delta E = \frac{1}{2} \cdot N \cdot \sum_{\gamma,\delta} \omega^{\gamma\delta} \sum_{i,j} e_{ij} \cdot \{y_{ij}^{\gamma\delta}(t + \Delta t) - y_{ij}^{\gamma\delta}(t)\}, \quad (8)$$

where  $\omega^{\gamma\delta}$  is the degeneracy factor of each pair which is equivalent to the coefficient of pair probability in eq.(1).  $X_{i,j}$ ,  $X_{j,kl}$  and  $W_{ijkl,mnop}$  are *path variables* for point, pair and tetrahedron clusters, which describe the time transition of the spin (atom) configuration on the sublattices specified in the sub- and superscripts, respectively. It is noted that path variables are the key configurational variables corresponding to cluster probabilities of the CVM.

In the PPF, the first term,  $P_1$ , describes the probability of non-correlated spin flipping (atomic exchange) events over the entire lattice points, the second term,  $P_2$ , is the thermal activation probability before and after the flipping (exchange) events, while the third term,  $P_3$ , which is similar to the configurational entropy of CVM given by the second term in eq.(1) describes the freedom of transition path. Then, PPM claims that the most probable path of the time evolution is determined so that the Path Probability Function is maximized, which is the variational principle corresponding to the minimization criterion of free energy in the CVM.

It is emphasized that the glass transition is driven by the enhanced viscosity with decreasing the temperature, which is not thermodynamic phenomenon but is essentially the kinetics phenomenon. In the PPF, the spin flipping probability  $\theta$  controls the elementary process of kinetics, and in the PPM studies of CG transition was assumed to be inversely proportional to the viscosity,  $\mu$ , given by

$$\theta = C \cdot \frac{1}{\mu}, \quad (9)$$

where  $C$  is a constant. Furthermore, in order to introduce the temperature dependence of the viscosity, following Vogel-Fulcher-Tamman equation[19] is assumed,

$$\mu = \mu_0 \exp\left(\frac{B}{T - T_K}\right), \quad (10)$$

where both  $\mu_0$  and  $B$  are materials constants.

One of the calculated cooling behavior of order parameters for three kinds of cooling rates are reproduced in Fig.2 [8]. The cooling rate  $R$  is normalized with respect to  $\theta \cdot \Delta t$ . One sees that as the ideal glass transition temperature ( $T_K = 0.861$  see Fig.1) is approached, the viscosity abruptly increases and the order parameter is gradually locked without proceeding to the equilibrium value predicted in the generalized phase diagram in Fig.1. This simulates the kinetics of glass transition.

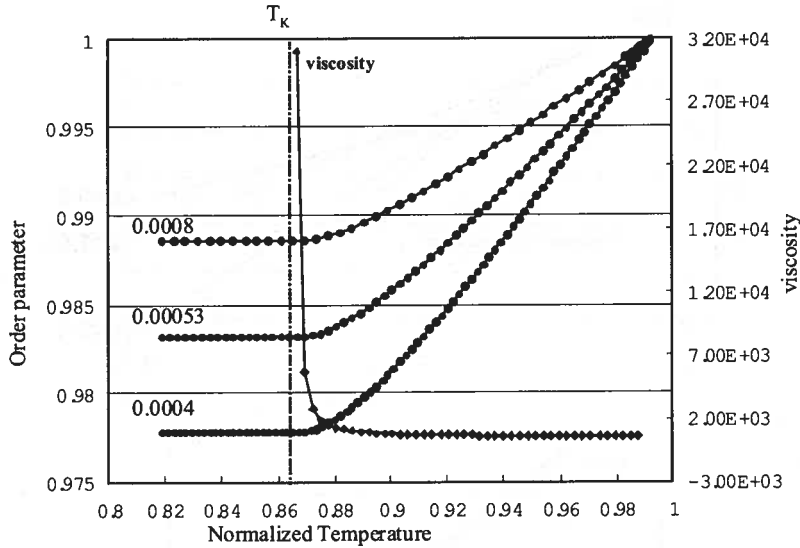


Fig. 2. Temperature dependences of order parameter at three kinds of cooling rate, 0.0008, 0.00053 and 0.0004. The initial state of the system is highly defective crystal just below the melting temperature. The temperature dependence of the viscosity in the present simulation is also indicated [8]

#### 4. Granato free energy model for glass transition

It was Granato [15] that provided one of the most versatile free energy expressions to describe the CG tran-

sition. The free energy is mathematically quite complicated with various materials parameters and is given by

$$y = x \cdot \left[ (1 - q) \cdot \left( \frac{1 - e^{-x}}{x} \right) + q \right] - tx \cdot \left[ 6\alpha\gamma \cdot \left( \gamma - \frac{1}{3} \right) \cdot \frac{G_0}{B} \cdot \left\{ (1 - q) \cdot \left( \frac{1 - e^{-x}}{x} \right) + q \right\} + \frac{4.35v}{1+ax} + \ln \frac{b}{x} - 4.25 \right]. \quad (11)$$

The above free energy formula was derived for fcc metals and Granato claimed this is a unified expression for crystalline, liquid and amorphous states. The basic idea behind this free energy expression involves the dielastic softening of shear moduli with defect concentration and, therefore, elastic moduli, vibrational frequency spectrum of a lattice etc. are taken into account. The main purpose of the present report is not to discuss the details of the free energy expression and readers interested in should refer to the original article. In the present context, it is suffice to focus only on the simplified expression of eq.(11) given by  $y = y(t, x)$  where  $t$  is the temperature and  $x$  is the amount of interstitialcies which may be regarded as the number of defects which induce the melting. This simplified expression is isomorphic to eq.(4) for the CVM free energy.

Among various quantities relevant to CG transition, ideal glass transition temperature is calculated based on eq.(11). The minimum of the free energy above the melting temperature,  $t_{melt}$ , corresponds to the liquid phase and the temperature dependence of the liquid free ener-

gy is plotted by a broken line in Fig.3(a). It is noted that the line intersects exactly at  $t_{melt}=1.0$  at which the free energy becomes 0, which is the energy reference state. Below  $t_{melt}$ , the liquid state is a metastable state. In the same figure, temperature dependences of free energies of three defective crystals characterized by  $x = 0.5, 1.0$  and  $2.1$  are plotted. The intersection of each curve with the broken line (liquid phase) indicates the melting temperature of a defective crystal. One sees that the melting temperature decreases with the increase of defects.

It is noticeable that the free energy curve of  $x = 2.1$  does not intersect but merges with liquid free energy at  $t = 0.86$ . (Note that Okamoto et al [20] was the first to perform the analysis but the present value slightly deviate from their results.) This suggests that the entropy of defective crystal of  $x^*=2.1$  and that of liquid becomes identical, which is the indication of the ideal glass transition temperature. In fact, the same analysis performed for the CVM free energy is demonstrated in Fig. 3(b) which should be realized as the vertical section of the free energy contour surface in Fig.1 evaluated at each  $\eta$ .

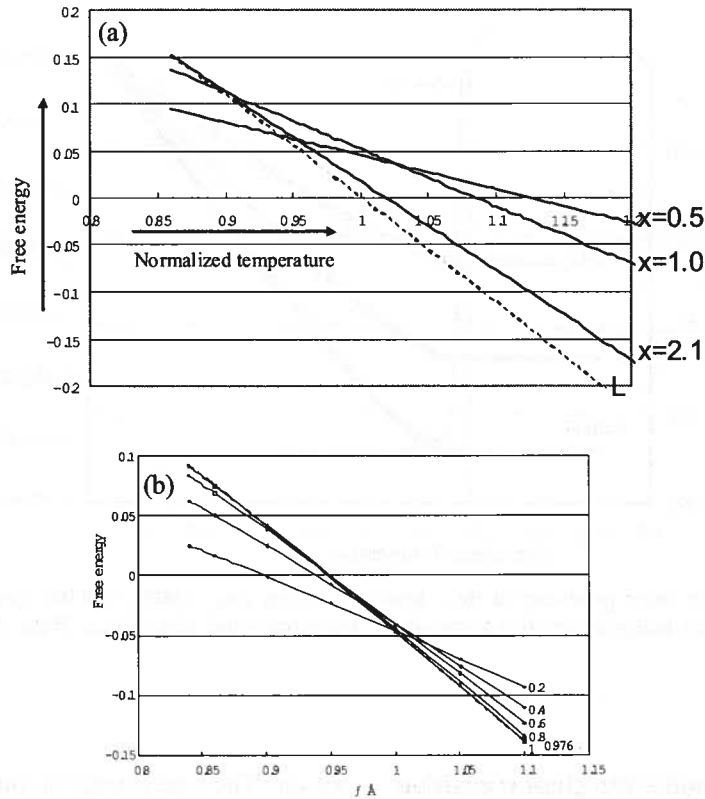


Fig. 3. (a) Temperature dependences of free energies for liquid (broken line), and three kinds of defective crystals characterized by the amount of the defect indicated by  $x$ . The free energy at  $x = 2.1$  no more makes intersection with liquid line but merges at  $t = 0.86$ . (b) The same analysis performed for CVM free energy. At 0.976, free energy merges liquid (1.0)

The merging of the free energies suggests the thermodynamic instability manifested by the vanishing of the second order derivative of the free energy, implying the loss of the stability against the fluctuation of the amounts of defects. As was pointed out in the previous section, this corresponds to the spinodal ordering in OD system. The clear distinction, however, should be made between CG transition and OD transition. The later can be discussed within the thermodynamics, while the former is mostly kinetics phenomena. Then, in order to study CG kinetics based on Granato free energy, a simple first order rate equation is employed,

$$\frac{\partial \eta}{\partial t} = -L \cdot \frac{\partial f}{\partial \eta}, \quad (12)$$

where  $\eta$  and  $f$  are the order parameter and the free energy which are equivalent to  $x$  and  $y$  in eq.(11), respectively, and  $t$  in the equation above is time which should not be confused with the temperature in eq.(11), and  $L$  is the relaxation constant. This rate equation is exactly the same as Time Dependent Ginzburg Landau equation without the gradient energy term. Since the elementary kinetics process is controlled by the relaxation constant, the enhancement of the viscosity with decreasing the temperature is accounted for through

$$L = D \cdot \frac{1}{\mu}, \quad (13)$$

where  $D$  is a constant and the temperature dependence of the viscosity  $\mu$  is again assigned through Vogel-Fulcher-Tamman equation [15] given by eq.(10).

The calculated cooling curves are demonstrated in Fig.4. In all the cases, the system is initially at temperature 1.2 (liquid state) and is cooled with three different cooling rates, CR, denoted in the figure, where CR=1.0 indicates that the system is cooled down to  $t = t_K$  (0.86) linearly with time steps 10000. CR=10, and 100 are ten and hundred times faster cooling rates, respectively. One clearly confirms the frozen of the order parameter ( $x$ ) for each cooling curve before reaching the critical defects concentration  $x^* = 2.1$ . Under the linear cooling rate, the bigger the CR is, quicker the reduction of relaxation constant due to the enhanced viscosity is encountered and the order parameter is frozen in the higher level of  $x$ .

As are understood from Figs.1 and 3(a) and (b), the appearance of the ideal glass transition temperature is a versatile property associated with a free energy curve for the first-order transition. Also, the locking of the order

parameter shown in Figs. 2 and 4 is a natural consequence of the retarding kinetics due to the exponential decay of thermal activation process.

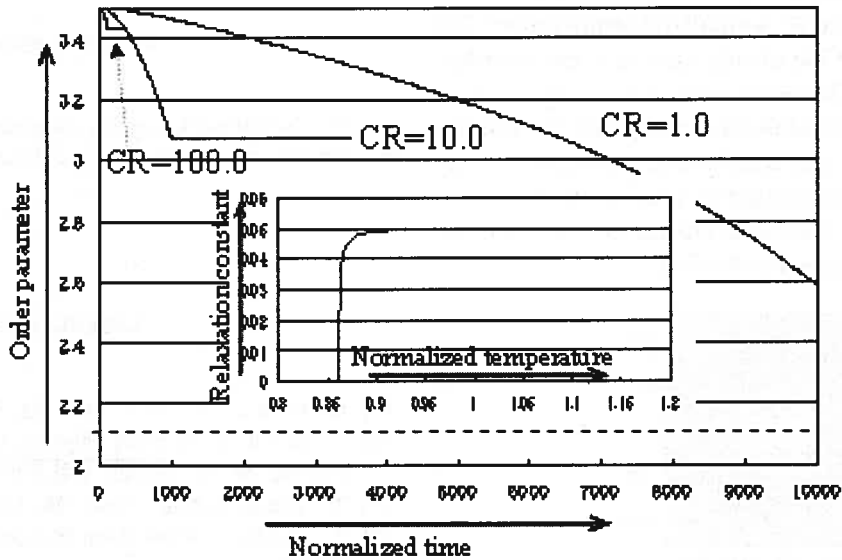


Fig. 4. Cooling curve obtained by Granato free energy. CR indicates the cooling rate and horizontal broken line indicates the critical amount of defects at the ideal glass transition temperature. Shown by insert is the temperature dependence of relaxation constant  $L$  assumed in the present study

Unlike Granato free energy which is based on sophisticated physical considerations of elastic properties, CVM free energies in eqs.(1) ~ (4) are merely an *analogue* to the first order thermodynamics. Yet, the natural extensibility to kinetics by PPM is a unique advantageous feature of the CVM, and it is desirable to explicitly incorporate structural properties of liquid and glass in the free energy. An attempt towards the incorporation of structural properties is briefly discussed within the Continuous Displacement CVM (CDCVM) in the next section.

## 5. Continuous Displacement Cluster Variation Method

The basic idea of the CDCVM [9-14] is to introduce additional points around each Bravais lattice point in order to allow an atom to displace to one of these points. These additional points are termed *quasi lattice points* and the additional freedom of the atomic displacements increases the entropy and reduces the internal energy, leading to the reduction of the free energy of the system. In particular, for a system with two atomic species in different atomic size, such displacements are enhanced and are detected by a scattering experiment [21].

Within the pair approximation of the CDCVM, the free energy is written as

$$\Psi = \omega \cdot \int d\mathbf{r} \cdot \int d\mathbf{r}' \cdot \varphi(|\mathbf{r} - \mathbf{r}'|) \cdot f_{pair}(\mathbf{r}, \mathbf{r}') - k_B \cdot T \cdot \left[ (2\omega - 1) \int d\mathbf{r} \cdot L(f_{point}(\mathbf{r})) - \omega \cdot \int d\mathbf{r} \cdot \int d\mathbf{r}' \cdot L(f_{pair}(\mathbf{r}, \mathbf{r}')) + (\omega - 1) \right], \quad (14)$$

where  $f_{point}(\mathbf{r})$  and  $f_{pair}(\mathbf{r}, \mathbf{r}')$  are point and pair distribution functions to describe the probabilities of finding an atom or an atomic pair, respectively.  $\mathbf{r}$  and  $\mathbf{r}'$  denote the displacement of an atom from the Bravais lattice point,  $\varphi(|\mathbf{r} - \mathbf{r}'|)$  is the atomic pair potential for which Lennard-Jones type potential is often assumed. It should

be realized this is the natural extension of the entropy formula of conventional CVM with the replacements of  $x_i$  by  $f_{point}(\mathbf{r})$  and  $y_{ij}$  by  $f_{pair}(\mathbf{r}, \mathbf{r}')$ . In the numerical calculations, the integral is replaced by sums and the number of meshes around a Bravais lattice point coincides with that of the quasi-lattice points. In the actual

minimization, two kinds of constraints originating from normalization condition imposed on the pair distribution function and symmetry requirements of the parents lattice are added to eq.(14). Shown in Figs. 5(a) and (b) are examples of the calculated point distribution function,  $f_{point}(\mathbf{r})$ , for the Lennard-Jones system on the two dimensional square lattice at normalized temperatures 0.3 and 1.0, respectively. One clearly sees that the distribution becomes sharper (broader) with decreasing (increasing) the temperature. In addition to the point distribution function,  $f_{point}(\mathbf{r})$ , the pair distribution function,  $f_{pair}(\mathbf{r}, \mathbf{r}')$ , conveys further information of local atomic structures. And, the bigger the basic cluster is, the more the structural information can be derived.

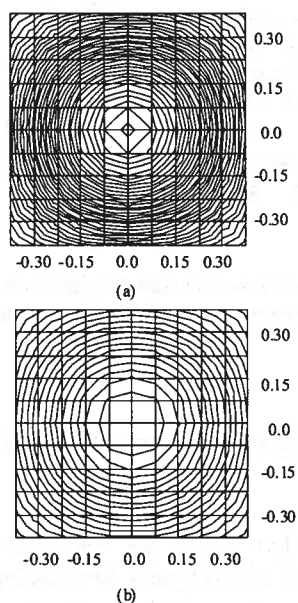


Fig. 5. Point distribution function around a Bravais lattice point of two dimensional square lattice at temperature 0.3 (a) and 1.0 (b). Temperature is normalized with respect to atomic interaction energy assigned by Lennard Jones potential. The numbers in the horizontal and vertical axes indicate the distance (1.0 corresponds to a lattice constant.) from Bravais lattice point at the center

The application of the CDCVM to CG transition is still at the beginning stage, and one of the basic necessities is to seek an appropriate order parameter. As was described, in most cases including conventional CVM, PPM and Granato free energy, the amount of the defects is commonly employed as the order parameter. In the CDCVM, a generalized Lindemann parameter [20] defined as

$$f = \frac{\langle (\bar{u})^2 \rangle^{1/2}}{a} \quad (15)$$

where  $\bar{u}$  the average atomic displacement and  $a$  the lattice constant, can be a candidate of the order parameter. In fact, a preliminary calculation [22] indicates that this approach is promising and more details will be published elsewhere.

#### Acknowledgements

The present work is partly supported by Next Generation Supercomputing Project, Nanoscience Program, MEXT, Japan.

#### REFERENCES

- [1] R. Kikuchi, Phys. Rev. **81**, 998 (1951).
- [2] T. Mohri, in Alloy Physics, Chapt. 10 and references therein, ed. W. Pfeiler, WILEY-VCH (2007), 525-588.
- [3] T. Mohri, Mat. Trans. **46**, 1180-1186 (2005).
- [4] T. Mohri, Trans. Mat. Res.Soc. of Japan, **30**, 885-887 (2005).
- [5] T. Mohri, Advanced Materials Research **26-28**, 723-726 (2007).
- [6] T. Mohri, Y. Kobayashi, Materials Science Forum **539-543**, 2425-2430 (2007).
- [7] R. Kikuchi, Prog. Theor. Phys. Suppl. **35**, 1 (1966).
- [8] T. Mohri, Y. Kobayashi, Materials Transaction **46**, 2811-2816 (2005).
- [9] R. Kikuchi, J. Phase. Equilibria **19**, 412-421 (1998).
- [10] R. Kikuchi, A. Beldjenna, Physica **A182**, 617 (1992).
- [11] R. Kikuchi, K. Masuda-Jindo, Comp. Mat. Sci. **14**, 295 (1999).
- [12] H. Uzawa, T. Mohri, Mat. Trans. **42**, 422 (2001).
- [13] H. Uzawa, T. Mohri, Mat. Trans. **42**, 1866 (2001).
- [14] H. Uzawa, T. Mohri, Mat. Trans. **43**, 2185 (2002).
- [15] A. V. Granato, Phys. Rev. Lett. **68**, 974 (1992).
- [16] R. Kikuchi, J. Chem. Phys. **60**, 1071 (1974).
- [17] D. de Fontaine, Acta metall. **23**, 553 (1975).
- [18] T. Mohri, J. M. Sanchez, D. de Fontaine, Acta Metal. **33**, 1463 (1985).
- [19] for instance, D. S. Sanditov, S. S. Badmaev, Sh. B. Tsydyrov, B. D. Sanditov, Glass Physics and Chemistry **29**, 2 (2003).
- [20] P. R. Okamoto, N. Q. Lam, L. E. Rehn, Solid State Physics **52**. ed. by H. Ehrenreich (Elsevier Academic Press, San Diego, 1999) and references therein.
- [21] T. B. Wu, J. B. Cohen, Acta metall. **32**, 861 (1984).
- [22] T. Kobayashi, ME dissertation, Graduate School of Engr., Hokkaido University, (2007).